

# Comparison of elastic electron or positron scattering from proton-rich nuclei\*

E. J. MA,<sup>1,2,3</sup> Y. G. MA,<sup>1,†</sup> J. G. CHEN,<sup>1</sup> X. Z. CAI,<sup>1</sup> D. Q. FANG,<sup>1</sup> W. GUO,<sup>1</sup> G. H. LIU,<sup>1</sup> C. W. MA,<sup>1</sup>  
W. Q. SHEN,<sup>1</sup> Y. SHI,<sup>1</sup> Q. M. SU,<sup>1</sup> W. D. TIAN,<sup>1</sup> H. W. WANG,<sup>1</sup> K. WANG,<sup>1</sup> and T. Z. YAN<sup>1</sup>

<sup>1</sup>Shanghai Institute of Applied Physics, Chinese Academy of Sciences, P. O. Box 800-204, Shanghai 201800

<sup>2</sup>Changshu Institute of Technology, Jiangsu 215500

<sup>3</sup>Graduate school of Chinese Academy of Sciences, Beijing 100039

(Dated: October 26, 2018)

We investigate the cross sections of the elastic electron or positron scattering from <sup>208</sup>Pb, <sup>12</sup>C, <sup>12,16</sup>O and <sup>28,32</sup>S by the relativistic partial-wave expansion method using the static charge density distribution from the self-consistent relativistic mean field model and also calculate the charge form factor for <sup>12,16</sup>O and <sup>28,32</sup>S. The numerical results are compared with the available data. Calculations indicate that the extended charge density distributions of <sup>12</sup>O and <sup>28</sup>S have observable effects on the cross sections of the electron or positron scattering as well as the charge form factors.

PACS numbers: 25.30.Bf, 21.10.Ft, 27.30.+t, 13.40.Gp

The use of radioactive nuclear beams (RNB) led to the discovery of neutron halo nuclei [1]. Besides neutron halo, another topic on halo nuclei is to search for proton halo from proton-rich nuclei. Theoretically, many calculations have been made to predict that there may be proton halos in <sup>26,27,28</sup>P [2], <sup>23</sup>Al, <sup>13</sup>N [3] etc. Although some measured data from experiments indicate some evidences of the existence of proton halos in these nuclei [4], further experiments are needed to confirm the existence of the proton halos. It is well known that the electron scattering off nuclei provides the most direct information about charge distribution. Technical proposals for an electron-heavy-ion collider has been incorporated in the GSI/Germany physics program [5] as well as the RIKEN/Japan facility [6]. In both cases the main purpose is to study the structure of nuclei far from the stability line. Since the electron-nucleus scattering is a better way for the precise investigation of the extended charge distribution and the experimental data for the electron scattering off unstable nuclei will be available soon, it is of interesting to make an exploratory investigation of elastic electron scattering from proton-rich nuclei.

There are some methods which can calculate the differential cross sections for the elastic high-energy electron scattering off nuclei. The conventional methods are the distorted wave Born approximation [7], the relativistic eikonal approximation [8] and the relativistic partial-wave expansion method [9]. The partial-wave expansion method is generally believed to be an “exact” method if enough partial waves are included in the phase-shift calculations. This method can deal with both electron and positron elastic scattering off nuclei, so we utilize it to

obtain the differential cross sections and form factors for electron or positron scattering off the exotic nuclei.

Some theoretical models can give reliable charge density distribution for stable nuclei. The typical models include the Skyrme-Hartree-Fork model [10], the ab initio no-core shell model [11], the large-scale shell model method [12] and the self-consistent relativistic mean field (RMF) model. A series of calculations [13, 14, 15, 16] show that the RMF model can reproduce with good precision the binding energies, the separation energies and the radii of nuclear charge density distribution. Therefore we use the RMF model to calculate the nuclear ground-state charge distribution.

The core of the relativistic partial expansion method is to solve a Dirac equation for the electron or positron in which the effect of the nucleus is contained entirely in the static Coulomb potential. We assume that the charge distribution of the target nucleus is spherically symmetric. The electrostatic interaction energy between the projectile and the target nucleus is

$$V(r) = Z_0 e \varphi(r), \quad (1)$$

where  $Z_0 e$  is the charge of the projectile ( $Z_0 = -1$  for electron and  $+1$  for positron) and  $\varphi(r)$  is the electrostatic potential of the target nucleus. Let  $\rho_{ch}(r)$  denotes the charge density of the target nucleus, we have

$$\varphi(r) = e \left( \frac{1}{r} \int_0^r \rho_{ch}(r') 4\pi r'^2 dr' + \int_r^\infty \rho_{ch}(r') 4\pi r' dr' \right). \quad (2)$$

The scattering of relativistic electrons or positrons by a central field  $V(r)$  is completely described by the direct scattering amplitude  $f(\theta)$  and the spin-flip scattering amplitude  $g(\theta)$  [17]. The elastic differential cross section in the relativistic partial-wave expansion method can be expressed as

$$\frac{d\sigma}{d\Omega} = |f(\theta)|^2 + |g(\theta)|^2. \quad (3)$$

After the differential cross sections are obtained, we can calculate the charge form factors  $F(q)$  by dividing the

\*Supported partially by the Shanghai Development Foundation from Science and Technology under Grant Numbers 05XD14021 and 06QA14062, the National Natural Science Foundation of China under Grant No 10328259, 10135030, and 10535010, and the Major State Basic Research Development Program under Contract No G200077404.

<sup>†</sup>Corresponding author. Email: ygma@sinap.ac.cn

differential cross sections with the Mott cross section  $(d\sigma/d\Omega)_{Mott}$  [18]

$$|F(q)|^2 = \frac{d\sigma/d\Omega}{(d\sigma/d\Omega)_{Mott}}. \quad (4)$$

Starting from Eq.(2), one can use Eqs.(3) and (4) to predict the differential cross section and the form factor for a given nuclear charge density distribution  $\rho_{ch}(r)$ .

To investigate the validity of the relativistic partial-wave method and the RMF model, we calculated positron or electron elastic scattering cross sections and their ratios for  $^{208}\text{Pb}$  and  $^{12}\text{C}$  for which the experimental data are available. In Fig.1, we show comparisons of electron

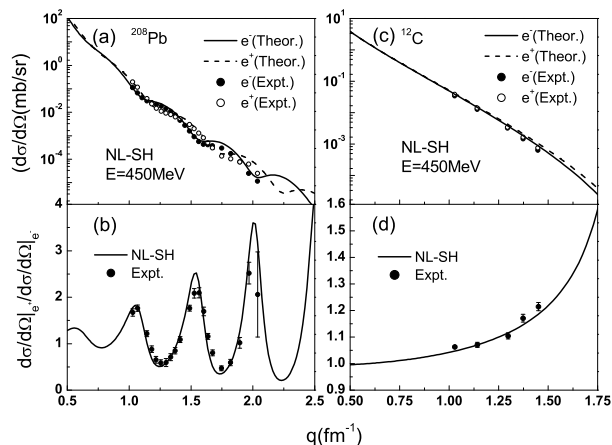


FIG. 1: Positron and electron elastic scattering cross sections and their ratios for  $^{208}\text{Pb}$  (left column) and  $^{12}\text{C}$  (right column).

and positron elastic scattering cross sections with the experimental ones [19] for  $^{208}\text{Pb}$  and  $^{12}\text{C}$  using a static charge density calculated by the RMF model with NL-SH parameters. The electron and positron are all leptons, but their electromagnetic interactions with nuclei are repulsive and attractive, respectively. So the Coulomb distortion of the electron or positron wave function by the scattering potential is different. The part of the Coulomb effect associated with the acceleration of the lepton by the Coulomb potential of the nucleus corresponds [20] to the effective momentum transferred between the lepton and the nucleus depending on the sign of the lepton's charge; this shifts the apparent location of the diffraction minima. The effects of the Coulomb distortion and the different effective momentum transfer are clearly visible in Fig.1(a); the locations of the diffraction minima are shifted between electrons and positrons due to the change in the effective momentum transfer, and the magnitudes of the cross sections at the same effective momentum transfer differ due to differences in the Coulomb distortion. Clearly, an electron-positron comparison is highly

sensitive to the Coulomb distortion effects, and the calculation is in general agreement with the measured data. Fig.1 also displays the theoretical cross sections and their ratios for  $^{12}\text{C}$  compared to the experimental data. The good agreement between experimental results and theoretical calculations for the  $^{12}\text{C}$  data is also reached.

For each incident energy and momentum transfer we determined the ratio  $R = (d\sigma/d\Omega)|_{e^+}/(d\sigma/d\Omega)|_{e^-}$  for both the measured data and the theoretical calculation. Fig.1(b) (d) displays theoretical and experimental values of  $R$  for  $^{208}\text{Pb}$  and  $^{12}\text{C}$ . The theoretical ratios are generally in good agreement with the measured ones[19].

From Fig.1, it indicates that the combination of the relativistic partial-wave method with the RMF model can give reasonable cross sections of high-energy electron or positron scattering off nuclei and the RMF model can produce the ground state charge density distribution of nuclei.

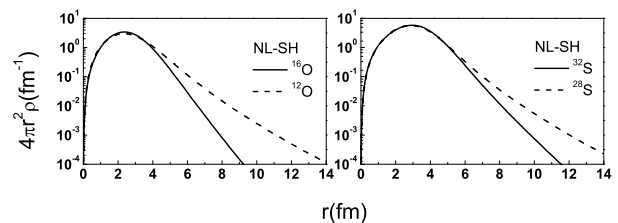


FIG. 2: The charge density distribution of  $^{12,16}\text{O}$  and  $^{28,32}\text{S}$  calculated with NL-SH force parameters in RMF model.

The charge density distributions of  $^{12,16}\text{O}$  and  $^{28,32}\text{S}$  are displayed in Fig.2. It is seen from Fig.2 that the charge density distributions of  $^{28,32}\text{S}$  with NL-SH parameters are different although the two nuclei have the same proton number. The weak binding of the last two protons in  $^{28}\text{S}$  leads to the extended charge density distribution in it. This agrees with the theoretical calculations [2], [16] and with the experimental results [4] of the neighboring nuclei  $^{26,27,28}\text{P}$ . The similar conclusion holds true for  $^{12,16}\text{O}$ .

In order to investigate the effect of the long tail of the charge density distribution of proton-rich nuclei on the process of elastic electron or positron scattering, the elastic scattering cross sections for the proton-rich nuclei  $^{28}\text{S}$  and  $^{12}\text{O}$  and respective stable isotopes  $^{32}\text{S}$  and  $^{16}\text{O}$  were calculated with the partial-wave method. Fig.3 displays the positron and electron elastic scattering cross sections and their cross section differences for  $^{12}\text{O}$  and  $^{16}\text{O}$  at different incident energies. The cross sections of the positron and electron elastic scattering off  $^{28,32}\text{S}$  for different incident energies are plotted in Fig.4. The difference of the cross sections  $D(q)$  in those figures is defined as

$$D(q) = \frac{(d\sigma/d\Omega)|_{e^-} - (d\sigma/d\Omega)|_{e^+}}{(d\sigma/d\Omega)|_{e^-} + (d\sigma/d\Omega)|_{e^+}} \quad (5)$$

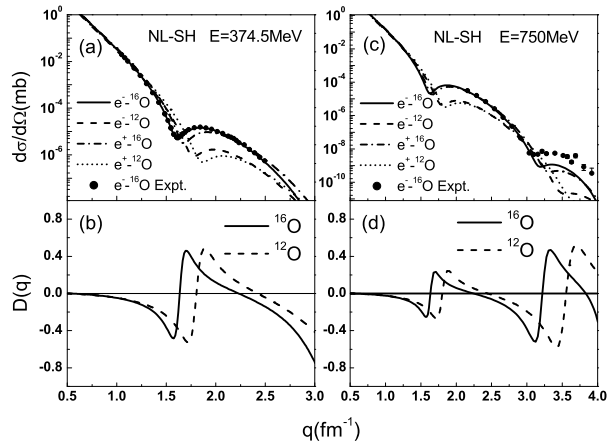


FIG. 3: Positron and electron elastic scattering cross sections and their cross section differences for  $^{12,16}\text{O}$ .

for electron- and positron-scattering from the identical nucleus. From those two figures, we can deduce the following conclusions.

Firstly, it is apparent that the calculated cross sections of electron scattering both for  $^{16}\text{O}$  and for  $^{32}\text{S}$  almost coincide with the experimental data [21, 22] in the range of low and moderate momentum transfer ( $q \leq 3\text{fm}^{-1}$ ). Theoretical results have very good agreements with the experimental data in this range of momentum transfer. At high-momentum transfers, a deviation occurs between the theoretical cross sections and the experimental data. Since the cross section in this range of momentum transfer is mainly sensitive to the details of the inner part of the charge density distribution [21], its occurrence indicates that the theoretical charge density distribution has a departure from the experimental one around the center of the nucleus. This means that the RMF model can reproduce the charge density distribution for  $^{16}\text{O}$  and  $^{32}\text{S}$  very well except near the center of the nucleus. The combination of the relativistic partial-wave method with the RMF model can predict the cross sections of the elastic electron-nucleus scattering from the stable isotopes of O and S.

Secondly, the cross sections of electron scattering from the unstable proton-rich nuclei  $^{12}\text{O}$  and  $^{28}\text{S}$  display the outward shifts of the positions of the diffraction minima as compared to the stable isotopes  $^{16}\text{O}$  and  $^{32}\text{S}$ . The differences of the cross sections both for  $^{12}\text{O}$  and  $^{16}\text{O}$  at the first minima of momentum transfer and for  $^{32}\text{S}$  and  $^{28}\text{S}$  at the second minima of momentum transfer are large enough to be observable in the experiments. On the one side, it can be deduced from the fitting to the experimental data of  $^{12}\text{C}$  [21] and  $^{32}\text{S}$  [22] that the cross sections in the range of moderate-momentum transfers, approximately  $1\text{fm}^{-1} \leq q \leq 3\text{fm}^{-1}$ , are sensitive to the tail of the nuclear charge distribution. On the other side, the weak binding of the last two protons in  $^{12}\text{O}$  and  $^{28}\text{S}$  leads

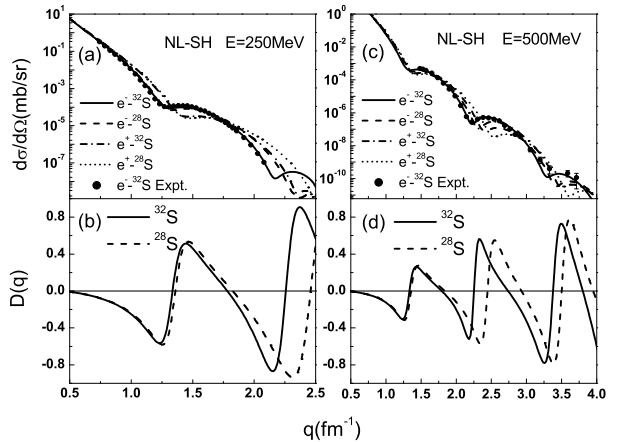


FIG. 4: Positron and electron elastic scattering cross sections and their cross section differences for  $^{28,32}\text{S}$ .

to the extended charge density distribution and the cross section of the elastic electron-nucleus scattering is related to the nuclear charge distribution. So the information of the long tail of the charge density distribution of  $^{12}\text{O}$  and  $^{28}\text{S}$  can be deduced by measurement of the cross sections of electron scattering from unstable proton-rich nuclei  $^{12}\text{O}$  and  $^{28}\text{S}$  at moderate-momentum transfers. Since the difference of the charge density distributions both for  $^{12}\text{O}$  and  $^{16}\text{O}$  and for  $^{28}\text{S}$  and  $^{32}\text{S}$  is mainly caused by the difference of the charge density distributions of the last two protons in  $^{12,16}\text{O}$  or  $^{28,30}\text{S}$ , the information of the density distribution of the last two protons could be extracted by comparing the cross sections of  $^{12,16}\text{O}$  or of  $^{28,30}\text{S}$ .

Thirdly, the cross sections of positron scattering from the stable nuclei  $^{16}\text{O}$  and  $^{32}\text{S}$  have the similar trends as compared with the ones of electron scattering from the same nucleus. Like the electron scattering from the unstable nuclei  $^{12}\text{O}$  and  $^{28}\text{S}$ , the positions of the diffraction minima of the cross sections of positron scattering from the unstable nuclei  $^{12}\text{O}$  and  $^{28}\text{S}$  shift outward in comparison to the positron scattering from the stable nuclei  $^{16}\text{O}$  and  $^{32}\text{S}$ . The difference between the cross section of positron scattering off the stable nucleus and the corresponding unstable isotope is apparent to be distinguishable in the positron-nucleus scattering experiment. So one can presume that the conclusions of analysis of electron-nucleus scattering still hold true for the positron-nucleus scattering, and the measurement and comparison of the cross sections of the positron scattering from unstable nucleus and the corresponding stable nucleus can provide the information of the ground-state charge density distribution of unstable proton-rich nuclei.

Fourthly, from analysis of the variation of the differences of the cross sections  $D(q)$  with momentum transfer, one can deduce that the locations of diffraction minima of the cross section for the positron-nucleus scattering are

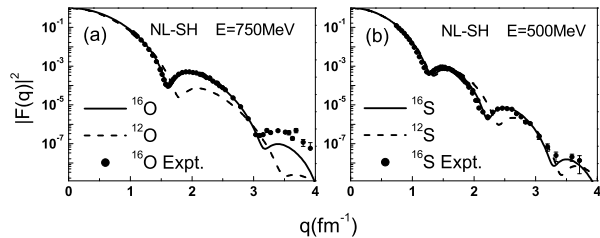


FIG. 5: The squared charge form factor for  $^{12,16}\text{O}$  and  $^{28,32}\text{S}$ .

shifted as compared with the electron-nucleus scattering. This shift is due to the different Coulomb effect of the target nucleus on electron and positron. The differences of the cross sections  $D(q)$  oscillate irregularly and the amplitudes of  $D(q)$  increase with momentum transfer. In the range of low momentum transfers, the solid curve (for  $^{16}\text{O}$  and  $^{32}\text{S}$ ) coincides with the dashed curve (for  $^{12}\text{O}$  and  $^{28}\text{S}$ ). This indicates that the differences of the cross sections between stable nucleus and corresponding unstable isotope can be observed in electron- or positron-scattering experiments only when the momentum transfers are larger than a certain value.

For the purpose of comparing the experimental data of electron-nucleus scattering at different incident energies, we calculated the charge form factor of  $^{12,16}\text{O}$  and  $^{28,32}\text{S}$ . Fig.5 displays the squared form factors of  $^{12,16}\text{O}$  and of  $^{28,32}\text{S}$ . The experimental cross sections for  $^{16}\text{O}$  and  $^{32}\text{S}$  are taken from Refs [21, 22]. The experimental cross sections at two different incident energies have been transformed into the squared form factors. It can be seen from Fig.5 that the location of the first minimum of the form factor of  $^{12}\text{O}$  and the position of the second minimum of the form factor of  $^{28}\text{S}$  shift outward markedly as compared with  $^{16}\text{O}$  and  $^{32}\text{S}$ . In addition, the amplitude of the form factor has a significant deviation, especially

in the neighborhood of the two minima. The shifts of the two minima and the amplitude deviation of the form factor are large enough to be observable. Since the form factor is connected to the charge density distribution by a Fourier transformation, the elastic electron scattering form factor of a nucleus is directly related to its charge density distribution which is mainly determined by the density distribution of protons in a nucleus. The weak-binding of the last two protons in  $^{12}\text{O}$  and  $^{32}\text{S}$  leads to the extended charge density distribution which results in the minimum shifts and the amplitude deviation of the form factors of  $^{12}\text{O}$  and  $^{28}\text{S}$  as compared with  $^{16}\text{O}$  and  $^{32}\text{S}$ . These effects should be observable and show that elastic electron-nucleus scattering can be used as an effective tool to study proton drip-line nuclei.

In summary, we have combined the RMF model with the relativistic partial-wave expansion method to investigate the elastic electron- or positron-nucleus scattering. Calculations indicate that the present theory is reliable for the elastic electron- or positron-nucleus scattering. The elastic electron or positron scattering cross sections and squared form factors of  $^{12,16}\text{O}$  and  $^{28,32}\text{S}$  are calculated and analyzed. In comparison to electron, positron scattering from a nucleus displays the minimum shift and the amplitude deviation of the cross section (in the same momentum transfer) that is due to the different Coulomb effect of a nucleus on positron and electron. As compared to the stable nuclei  $^{16}\text{O}$  and  $^{32}\text{S}$ , both the shifts of the minimum and the amplitude deviations of the cross section or the form factors of  $^{12}\text{O}$  and  $^{28}\text{S}$  result from the existence of the long tail of the charge distribution which is essentially attributed to the influence of the charge density distribution of the last two protons in  $^{12}\text{O}$  and  $^{28}\text{S}$ . Since the difference of the cross sections and form factors between a stable nucleus and its proton drip-line isotopes is large enough to be experimentally observable, the elastic electron- or positron-nucleus scattering is an effective tool to investigate proton-halo phenomena of proton-rich nuclei.

- 
- [1] I. Tanihata et al. 1985 Phys. Rev. Lett. **55** 2676  
[2] B. A. Brown et al. 1996 Phys. Lett. B **381** 391; Z. Ren et al. 1996 Phys. Rev. C **53** R572  
[3] H. Y. Zhang et al. 2003 Nucl. Phys. A **722** C518  
[4] A. Navin et al. 1998 Phys. Rev. Lett. **81** 5089; H. Y. Zhang et al. 2002 Nucl. Phys. A **707** 303; X. Z. Cai et al. 2002 Phys. Rev. C **65**, 024610; Z. H. Liu et al. 2004 Phys. Rev. C **69**, 034326  
[5] Haik Simon 2005 *Technical Proposal for the Design, Construction, Commissioning, and Operation of the ELISE setup* (GSI Internal Report, Dec. 2005)  
[6] T. Suda et al. 2001 *Proposal for the RIKEN beam factory, RIKEN, 2001*; M. Wakasugia et al. 2004 Nucl. Inst. Meth. Phys. A **532** 216  
[7] A. N. Antonov et al. 2005 Phys. Rev. C **72** 044307  
[8] Z. Wang et al. 2004 Phys. Rev. C **70** 034303  
[9] D. R. Yennie, D. G. Ravenhall, and R. N. Wilson 1954 Phys. Rev. **95** 500  
[10] W. A. Richter et al. 1954 Phys. Rev. C **67** 034317  
[11] M. A. Hasan et al. 2004 Phys. Rev. C **69** 034332  
[12] S. Karataglidis et al. 1997 Phys. Rev. C **55** 2826  
[13] Y. K. Gambhir et al. 1990 Ann. Phys. (N.Y.) **198** 132  
[14] C. J. Horowitz et al. 1981 Nucl. Phys. A **368** 503  
[15] Z. Ma et al. 1994 Phys. Rev. C **50** 3170  
[16] Z. Ren et al. 1999 Nucl. Phys. A **652** 250  
[17] D. W. Walker 1971 Adv. Phys. **20** 257  
[18] R. Hofstadter 1956 Rev. Mod. Phys. **28** 214  
[19] V. Breton et al. 1991 Phys. Rev. Lett. **66** 572  
[20] D. R. Yennie et al. 1965 Phys. Rev. **137** B882  
[21] I. Sick et al. 1970 Nucl. Phys. A **150** 631  
[22] G. C. Li et al. 1974 Phys. Rev. C **9** 1861